DETERMINISTIC PROPAGATION MODEL INFLUENCE ON A WIRELESS DIGITAL TRANSMISSION SIMULATION IN REAL ENVIRONMENT

Pierre Combeau, Lilian Aveneau, Rodolphe Vauzelle, Christian Chatellier

SP2MI, Téléport 2, Bd Marie et Pierre Curie, BP 30179, 86962 FUTUROSCOPE CHASSENEUIL Cedex, France
combeau@sic.sp2mi.univ-poitiers.fr

Abstract - The purpose of this paper is to describe the results of a CDMA digital transmission simulation in terms of quality, based on deterministic modeling of the propagation channel. This modeling allows a fast computation of the channel Power Delay Profile (PDP), which is the common input of a digital transmission system. Thus, the harmful impact of the channel is shown under the original form of Bit Error Rate (BER) maps. Such a representation becomes possible because of our propagation model efficiency, particularly compared to a ray tracing one. These maps represent a part of the Poitiers University in France.

Keywords - Propagation model, digital transmission system, bit error rate, error correcting code, CDMA.

I. INTRODUCTION

For a simulation of a digital transmission, normalized models are often used to simulate the propagation channel. Although they are very simple to implement, they stay very approximative and do not allow to correctly evaluate the channel influence on the transmission quality in different environments.

Recently, the lightning rise of radio mobile systems led to the development of very effective deterministic propagation models. Indeed, new radio mobile systems require an accurate knowledge of the channel behaviour for multimedia applications. Deterministic propagation models based on the Uniform Theory of Diffraction (UTD) and ray tracing [1] have emerged as dominant techniques to solve this problem. So it is now possible to study the behaviour of a digital transmission simulation in real conditions.

In this paper, we propose an original study endeavouring to describe the quality evolution of a CDMA radio link using an deterministic propagation model. Our approach is based on UTD and so give the same results that ray tracing methods, while presenting very smaller computation times.

The presentation of this work is organized as follows. In section II, the authors summarize the CDMA transmission chain. Section III first presents our deterministic model based on Optical Geometry (OG) and Uniform Theory of Diffraction (UTD), and secondly a comparison study with a ray tracing one in terms of computation times. Section IV illustrates its impact on the transmission quality. It shows the BER evolution in function of the path number taken into account in the PDP to characterize the importance of an accurate model versus a statistical one. This last one considers only some arbitrary paths. Then, an application is depicted considering a JPEG picture transmission firstly without any protection, and secondly with a Reed Solomon Error Correcting Code (ECC).

II. THE CDMA TRANSMISSION CHAIN

The transmission chain is based on the CDMA procedure which the general structure is presented on figure 1.

A. Principle

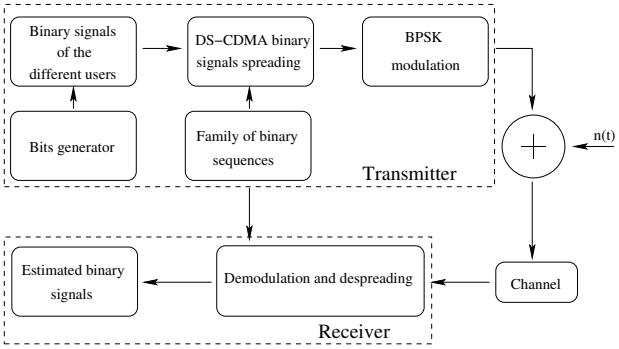

FIG. 1. The implemented transmission chain

The user binary signal is generated by a simple bit random generator. Then, a spectral spreading is realized with a particular binary sequence. Thus the spreading signal becomes more robust to multipaths phenomena and interuser interferences. The spreaded signal is then transmitted with a BPSK modulation on the considered channel. The link noise is characterized by an Additive White Gaussian Noise (AWGN).

The multi path channel is simulated by a Tapped Delay Line (TDL) filter. This filter is sampled at time chip (Tc) rate, allowing to treat different paths by multiple step of Tc.

Despreading is realized by multiplying the received signal at channel output by the used sequence. This allows to only

recover the spectral component corresponding to the spreaded signal by this same sequence. Furthermore it spreads all wideband noises present on the link (the other users' signals). Finally, a Rake receptor has been implemented.

B. The channel modeling

If we consider a stationary channel, its impulse response is given by :

$$\tilde{c}(t) = \sum_{k=1}^{k=N} \tilde{a}_k \delta(t - \tau_k) \quad (1)$$

where $\tilde{a}_k$ is the complex coefficient of the path k. If $\tilde{s}(t)$ is the transmitted signal and $\tilde{r}(t)$ the received one, we obtain :

$$\tilde{r}(t) = \sum_{k=1}^{k=N} \tilde{a}_k \tilde{s}(t - \tau_k) \quad (2)$$

In this case, the channel is modeled by a TDL filter (figure 2).

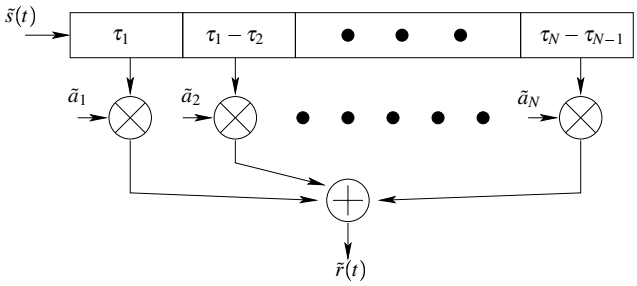

FIG. 2. TDL filter

III. DETERMINISTIC PROPAGATION MODEL

Its purpose is to build the channel impulse response $\tilde{c}(t)$ in real environments. This model is an extension of previous works [2][4] which have been developed for a narrow band study of the channel in microcellular configurations. It is based on a spatial partitioning of the propagation environment.

As it has been shown in literature, in a microcellular configuration a horizontal 2D propagation study is sufficient [3]. So, the proposed method is developed in such a plane. It splits up into two steps :

- Construction of a tree containing the zones
- Computation of the paths

A. Construction of a tree of zones

Since we are in 2D, we consider that a building face becomes an edge, and a building edge a vertex. Then, the first step consists in partitioning the propagation environment [4] into three types of geometrical zones : visibility, reflection and diffraction zones, respectively depicted at figure 3 (a), (b) and (c).

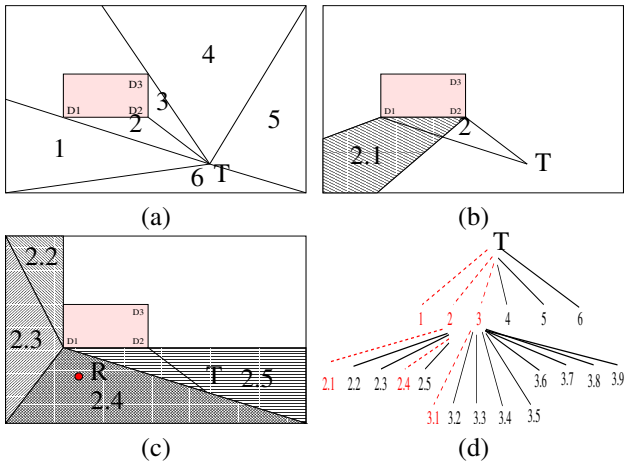

FIG. 3. Construction of : (a) the visibility zones, (b) the reflection zone on face D1D2, (c) the diffracted zones at D1, (d) the zone tree

Each zone is either a triangle or a quadrangle, and finishes either on a building edge or on one side of the studied area. This principle is illustrated on the figure 3 (a) for the visibility zones marked 1 to 6. All these zones represent the first level of the tree. Each of them can have children, *i.e.* zones associated to either reflection phenomenon on edges, or diffraction on building vertices. For instance, the zone marked 2 in the figure 3 (a) produces three new zones :

- a reflected one on the edge D1D2 (figure 3 (b))
- a diffracted one on the vertex D1 (figure 3 (c)).
- a diffracted one on the vertex D2 (not shown on the figure).

Notice that, like for the visibility zone, the children zones are cut in either several quadrangles or several triangles. In figure 3, zone 2 leads to zones labeled as 2.1 to 2.5. Considering zone 3, the children are either reflected on edge D2D3 (zone 3.1), or diffracted on vertices D2 and D3 (zones from 3.2 to 3.9) after triangulation (these zones are not depicted on the figure).

It is important to underline that choosing diffraction scatters can turn up to be difficult at a same tree level. For instance, at the second one, it is possible to diffract at vertex D2 from both zone 2 and zone 3. Of course, the diffraction at D2 must be calculated only once. To solve this problem, we put a label on each vertex and for each tree level. In our example, after having diffracted once at the vertex D2 from zone 3, D2 is already labeled, and then no more diffraction from zone 2 is computed. So each diffracted path at each tree level is computed only once.

As for a ray tracing method, the main parameter to compute the tree is the number N of considered electromagnetic interactions (reflection and diffraction) ; N gives the depth of the tree. For one diffraction and one reflection (N = 2), the

resulting tree is shown on figure 3 (d).

Finally, notice that the tree computation is made only once, whatever the position of the receiver in the studied area is. Clearly this allows to largely optimize the computation time.

B. Path computation

When the tree has been computed, we can build the paths between the transmitter and a receiver ; this is an easy step using a discrete geometrical algorithm in a way similar to [4]. The first phase consists in determining all zones that include the receiver location. The simplest way is to do this "including test" for all zones ; of course, too many zones leads to heavy computation times. Our method reduces the number of such tests by first plunging all zones in a discrete grid. From there, we directly know what zones are in a given grid element. So for each receiver location, we compute its corresponding grid element ; then, we do the including test only for zones which are plunged in the same grid element. This leads to an important optimization in terms of computation time.

Now, we can compute the paths corresponding to the zones which include the receiver location. We only have to traverse the tree from the receiver to the root. Notice that each branch from the receiver location in the tree to the root corresponds to an exact propagation path. Indeed, unlike ray tracing methods, no visibility test is necessary to validate the path. This allows to reduce again computation time. For instance, figure 3 (d) shows the computation of the different paths by traversing the tree from a receiver R to a transmitter T (dashed lines). Finally, the path loss computation is provided by a classical method based on Geometrical Optic and on the Uniform Theory of Diffraction[5].

To provide computation time evaluations, we present results on a scene corresponding to a dense urban environment in microcellular configuration, the roundabout of *Arc de Triomphe* in Paris, France (depicted in [4]). The dimension of this scene is 1162x1364 meters. It includes 813 buildings *i.e.* 9516 edges and vertices. Table I shows the evolution of computation time for a receiver in this environment according to the interaction combination, for a classical 2D ray tracing method and for ours. Notice that the computed impulse responses are the same for both methods. For ours, we give computation time for the tree construction and for the path computation. For this study, all computations have been obtained with an Athlon XP 1800+.

TAB. 1. Comparison for one receiver location

Interactions	Classical 2D ray tracing	Our Method	
		Tree	Path computations
1R−1D	4 mn	14s 41	0s 18
2R−1D	55 days	37s 85	0s 56
3R−1D	———	1mn 18s 98	1s 89
4R−1D	———	2mn 25s 5	2s 76

Obviously, our method is largely faster than a classical 2D ray tracing whatever the combination of interactions is. Moreover, we can notice that the calculation is not acceptable (more than 55 days) for the classical ray tracing from 2R, whereas our method leads to a computation time that roughly equals one minute. So our method allows to consider complex combinations of interactions for very dense environments, which is impossible for a classical ray tracing. To conclude, this model presents the advantages of a ray tracing model while minimizing its drawbacks.

IV. RESULTS AND DISCUSSION

In this section, we show how fine characterization of the radio channel can influence the transmission quality. All given results concern the same scene which is a part of the Poitiers University. This one is depicted on figure 4 and illustrates a microcellular configuration.

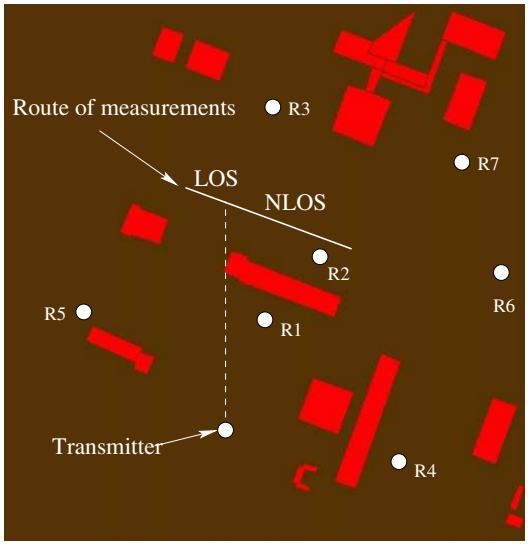

FIG. 4. A part of the university of Poitiers campus

White points indicate the locations of the transmitter and seven particular receivers (R1 to R7), buildings are represented in red. To characterize the propagation channel, and the transmission quality, we first compute the PDP. As an example, figure 5 shows the evolution of the PDP on the route of measurements depicted on figure 4.

Then, we can compute wideband parameters such as the RMS delay spread or the coherence bandwidth, or even characterize the doppler effect. Because our channel modeling is very fast, we can compute the PDP in the whole studied environment and deduce from it the delay spread map presented on figure 6. For this, we have computed it on a discrete grid and chosen a step of 2 meters between each receiver. In accordance to theory, the RMS goes from very low values (0 ns) in visibility zones to a few hundreds of nanoseconds in

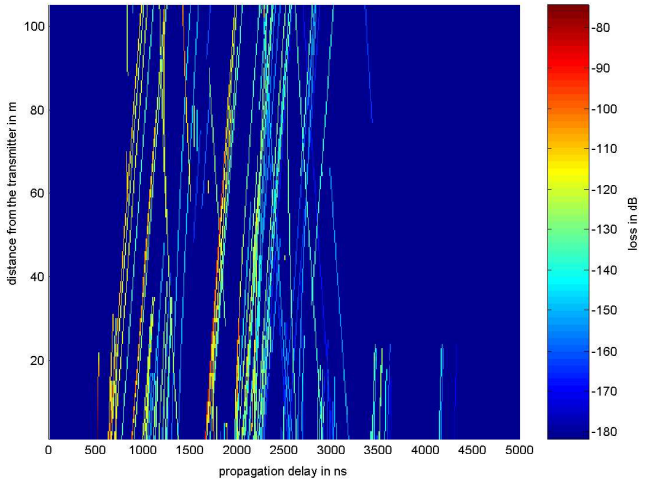

FIG. 5. PDP evolution on the route of figure 4

building shadow ones. This parameter is very interesting for the transmission quality evaluation, because theory indicates that when it is higher than Tc, there is a high risk of intersymbol interferences.

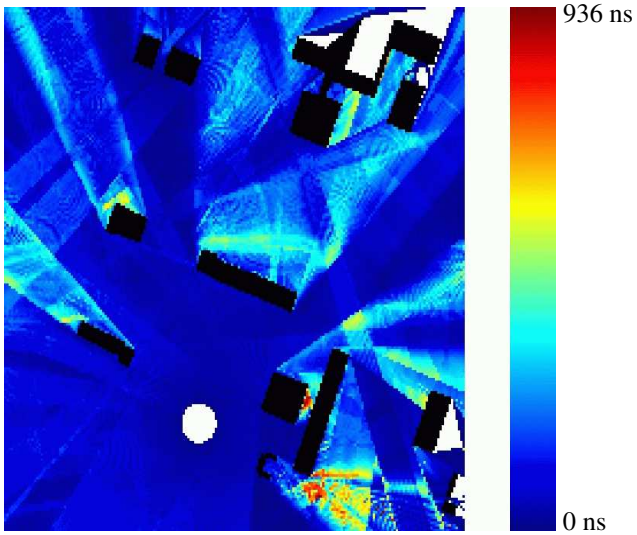

FIG. 6. Delay Spread map in the studied environment

For our digital transmission simulations, we consider one user who transmits a message of 500 000 bits randomly generated. Since there is only one single user, there will be no interuser interferences and the choice of the binary sequence is not important. So, we also randomly generate it. SNR has been fixed to 13, spreading factor to 2 and bit flow to 4 Mbit/s.

One can notice that all paths found in the PDP (figure 5) are not significant. So we propose a study which describes the evolution of the BER in function of the path number taken into account in the PDP. This study will be used to determine the optimal number of fingers to take into account in a Rake receiver. Notice that paths are eliminated by crescent order : it means that we first eliminate the most lossy paths. This study concerns the seven receiver locations depicted on figure 4. Results are shown on figure 7.

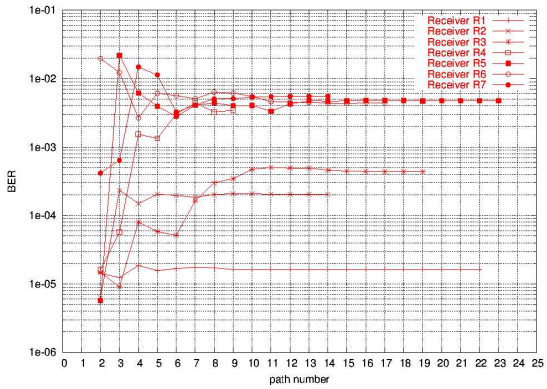

FIG. 7. BER evolution according to the path number

We can notice that according to the PDP introduced in the TDL filter, the BER is significantly modified. As an example, the BER at the receiver R3 goes from 8×10^{-5} for 4 paths, to 5×10^{-4} for 11 paths. Furthermore, even with a very small number of paths, as in classical statistical models, BER values can be very unstable. Thus for R5, the BER goes from 2×10^{-2} to 6×10^{-3} between PDP with 3 and 4 paths. Finally, one can notice that the BER becomes stable when we reach about seven paths, which is higher than the classical four paths statistical models. These results show the importance of an accurate channel modeling.

Now, as a global result, let's see the BER map of the studied environment on figure 8.

In this map, the BER goes from 0 for the LOS locations to 2.12×10^{-1} for some NLOS ones.

Figure 9 shows the cumulative function of the BER values (in solid line) and indicates that 90% of receivers have a BER smaller than 2×10^{-2} and 73% smaller than 10^{-3}. Obviously, the receiver locations corresponding to the maximum values of BER are in the bulding shadow zones, and correspond to the high values of RMS delay spread. Again, this result confirms the theory. Furthermore, notice that this diversity is not explicitly studied by a normalized channel, indeed this one would be constant for all receiver locations.

Now it would be interesting to study the influence of the propagation channel on a protected information transmission. To do this, we use a classical Reed Solomon code, with a code rate of 1.13. The cumulative function corresponding to the same map that the one of figure 8 but with ECC is shown on figure 9 in dashed line. One can observe the very powerful effect of ECC which corrects errors until a BER values of 10^{-2}. Indeed, whereas there were 47% of receivers with a

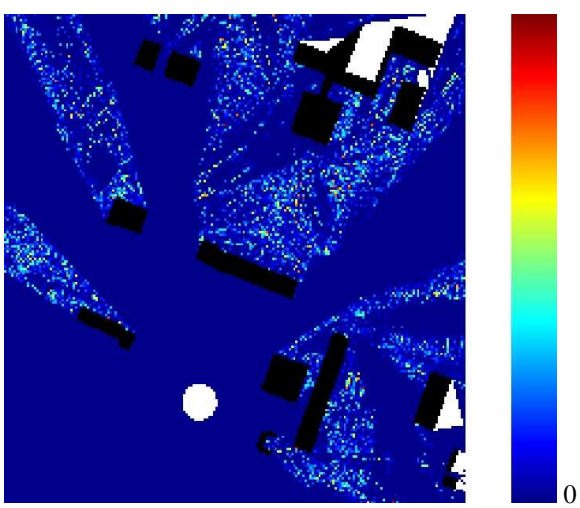

FIG. 8. BER map for the studied environment

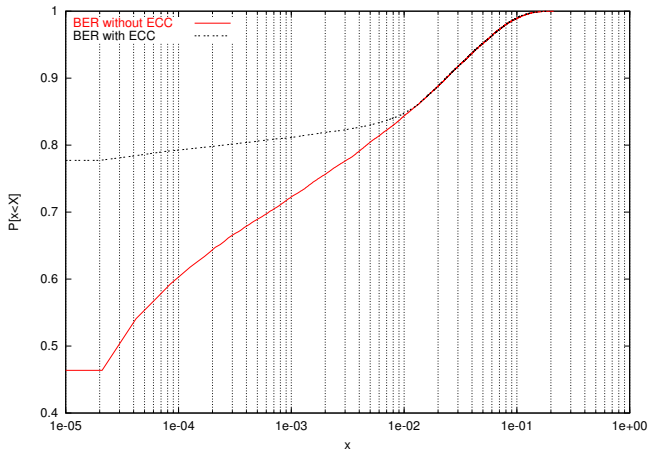

FIG. 9. Cumulative function of the BER values

BER smaller than 2×10^{-5} without ECC, they are 78% with ECC.

Finally, we propose as conclusion a transmission example of an image through our simulator. We have chosen the test image Lena in greyscale and compressed in JPEG format with a compression rate of 8. Figure 10 shows the received image at the receiver R5 with ECC.

How one can observe on this figure, even with ECC several receiver locations present a harmful impact of the channel which do not allow to restore the right information.

V. CONCLUSION

In this paper we have presented an efficient deterministic propagation model to study the channel influence on a wireless digital transmission. We have shown that, with acceptable computation time, it is possible to compute the PDP on a large geographic zone and determine all parameters characterizing local channel behaviour on geographic maps. Such representation can give precious informations to calibrate digital transmission systems, particularly the number of fingers to take into account in a Rake receiver. Finally, we have shown that classical statistical models are insufficient to accurately study the transmission quality in real environments.

FIG. 10. Received image with a Reed Solomon code rate of 1.13

THANKS

These works have been developed with the financial support of the *région Poitou Charentes*.

REFERENCES

[1] F. Escarieu, Y. Pousset, L. Aveneau, and R. Vauzelle. Outdoor and indoor channel characterization by a 3d simulation software. PIRMC, San Diego, 2001.

[2] Y. Pousset, R. Vauzelle and P. Combeau. Optimizing the computation time of radio coverage predictions for macrocellular mobile systems. *IEE Proceedings. Microwave and Antennas Propagation*, to be published.

[3] K. R. Schaubach, N. J. Davis IV, and T. S. Rappaport. A ray tracing method for predicting path loss and delay spread in microcellular environments. *IEEE Vehicular and Technology Conference*, pages 932–935, Denver, May 1992.

[4] L. Aveneau, P. Combeau, R. Vauzelle, and M. Mériaux. Efficient computation of radio coverage zone using a spatial partitionment approach. *IEEE Vehicular and Technology Conference*, Orlando, October 2003.

[5] R. G. Kouyoumjian and P. H . Pathak. A uniform geometrical theory of diffraction for an edge in a perfectly conducting surface. *Proc. IEEE*, pages 1448–1461, November 1974.